Biomedical Signal Processing and Control 32 (2017) 150–156

Contents lists available at ScienceDirect

Biomedical Signal Processing and Control

journal homepage: www.elsevier.com/locate/bspc

Inertial sensor and cluster analysis for discriminating agility run technique and quantifying changes across load

Ryan S. McGinnis[a,*], Stephen M. Cain[b], Steven P. Davidson[c], Rachel V. Vitali[b], Scott G. McLean[c], Noel C. Perkins[b]

[a] Electrical and Biomedical Engineering Department, University of Vermont, Burlington, VT 05405, USA
[b] Mechanical Engineering Department, University of Michigan, Ann Arbor, MI, USA
[c] Kinesiology Department, University of Michigan, Ann Arbor, MI, USA

ARTICLE INFO

Article history:
Received 24 November 2015
Received in revised form
10 September 2016
Accepted 25 October 2016
Available online 31 October 2016

Keywords:
Inertial measurement units
Optimization
Drift correction
Human performance
Agility
Load carriage

ABSTRACT

Performance in an agility run drill is often used to characterize an athlete's ability to quickly and explosively change direction. Beyond athletic applications, agility tasks are also used to assess the physical readiness of warfighters for battle and the influence that their equipment has on their performance. However, in all of these applications, performance is currently assessed solely by the time it takes to complete the drill. While completion time meaningfully discriminates bottom-line performance, it does not reveal the underlying biomechanics that contributes to or limits that performance. Biomechanical metrics that accurately identify performance strengths and weaknesses could promote rapid performance gains via tailored training programs and inform equipment design. To these ends, we propose a belt-worn wireless inertial measurement unit (IMU) to quantify biomechanical metrics underlying speed and agility performance in agility tasks. A drift correction methodology is introduced that yields estimates of displacement, velocity, and acceleration of a subject's sacrum in a course with known waypoints. We apply this methodology on a large data set collected from 32 subjects completing a slalom run with and without a 20.5 kg load. A k-means cluster analysis of proposed performance metrics reveals two groups of subjects who use fundamentally distinct techniques to negotiate the turns of the course in the unloaded condition. The groups exhibit different adaptations following application of the load, ultimately erasing group differences in the loaded condition. We believe that this measurement methodology can be used widely for agility assessment to provide athletes, trainers and researchers with actionable data to inform training plans and equipment modifications.

1. Introduction

A deep understanding of warfighter and emergency responder fitness and the effects of equipment is paramount for maximizing performance and safety. Obstacle courses that incorporate a variety of functional tests are often used to assess fitness and for designing equipment [1]. One such obstacle course is the Marine Corps Load Effects Assessment Program (MC-LEAP), which includes sprinting, jumping, and balance tasks as well as a slalom run to assess agility performance and the associated effects of equipment and load. Significant work has been done to characterize the influence of load carriage on the biomechanics of gait, balance, and jumping [2–6], but little has been done to extend these analyses to agility and the associated assessment tasks.

Agility is defined as "a rapid whole body movement with change of velocity or direction in response to a stimulus" [7]. Therefore, agility is decomposed into two distinct tasks: (1) perception and interpretation of a stimulus, and (2) rapid biomechanical reaction to that stimulus through a change of direction or velocity. Success in both of these tasks is required for superior agility performance. Agility run drills are commonly used to test a subject's ability to quickly and explosively change direction [7]. However, performance in these tests is currently assessed solely by reporting the time it takes to complete the drill. While completion time meaningfully discriminates bottom-line performance, it does not reveal the underlying biomechanics that contributes to or limits that performance.

* Corresponding author.
E-mail addresses: ryan.mcginnis@uvm.edu (R.S. McGinnis), smcain@umich.edu (S.M. Cain), stevepd@umich.edu (S.P. Davidson), vitalir@umich.edu (R.V. Vitali), mcleansc@umich.edu (S.G. McLean), ncp@umich.edu (N.C. Perkins).

http://dx.doi.org/10.1016/j.bspc.2016.10.013
1746-8094/

Human biomechanics are often quantified using video-based methods where a subject is tracked by a system of cameras that capture the motion of skin-mounted reflective markers (see validation of [8], for example). However, video methods typically require expensive camera systems, skilled operators, and significant data reduction and post processing before meaningful information can be generated. These limitations restrict their use to highly controlled (often laboratory) settings which prevents wide adoption by athletes, trainers, coaches, researchers, and equipment designers.

Recent advances in miniaturized inertial measurement units (IMUs) have enabled accurate measurement of human biomechanics without the constraints imposed by video-based systems and at a fraction of the cost [6,9–13]. These devices have been used to study the temporal characteristics of sprint running [11,12] however, IMUs are limited in their ability to estimate spatial characteristics, as doing so requires an error-prone double integration of acceleration [14]. In the study of human ambulation, this limitation is often overcome by mounting a device to the foot of a subject and utilizing established pedestrian localization methods to extract the trajectory of the foot [8]. However, foot trajectory data alone does not describe the motion of a subject's mass center which represents whole-body movement. The motion of the subject's mass center is reasonably approximated by that of the sacrum. The sacrum trajectory can be reconstructed from data from multiple sensors along the kinematic chain of the legs originating from a ground contact point [15]. However, the reliance on multiple sensors increases experimental complexity and reduces the likelihood of translation outside of research contexts.

A new method, first introduced by the authors in [16] and expanded in detail herein, employs a single, belt-worn IMU for quantifying the kinematics of the sacrum during drills that assess agility performance. The kinematical measures, including the sacrum trajectory, velocity, acceleration, orientation, and angular velocity, follow from a new drift correction algorithm. We demonstrate our method on a large dataset of 32 subjects, and we observe they employ two distinct turning techniques while completing a slalom run. We then examine how the two groups adapt their techniques to compensate for the application of a 20.5 kg load.

2. Methods

2.1. Human subject testing

Thirty-two subjects were recruited for participation in this study from the local university population. Prior to testing, informed consent was obtained from each participant and the testing protocol was approved by the University of Michigan Institutional Review Board. Testing began with subjects executing a simple calibration routine that included standing still with an upright posture, walking in a straight line, and touching the toes. Following calibration, each subject was instructed to complete a slalom run course as quickly as possible starting from rest. The slalom course, illustrated in Fig. 1, was composed of seven cones spaced 5 m apart to define five changes of direction. Subjects completed the course at maximal effort once each in a loaded and unloaded condition. The load condition applied first was randomly selected. During the loaded condition, subjects wore the US Army's Improved Outer Tactical Vest (IOTV) with Enhanced Small Arms Protective Insert (ESAPI) training plates and the Tactical Assault Panel (TAP), and the IOTV without the training plates or panel in the unloaded condition. In both cases, subjects carried a mock rifle designed to have similar weight (3.4 kg) and dimensions to a standard M4 rifle. The difference in mass between loaded and unloaded conditions was approximately 20.5 kg.

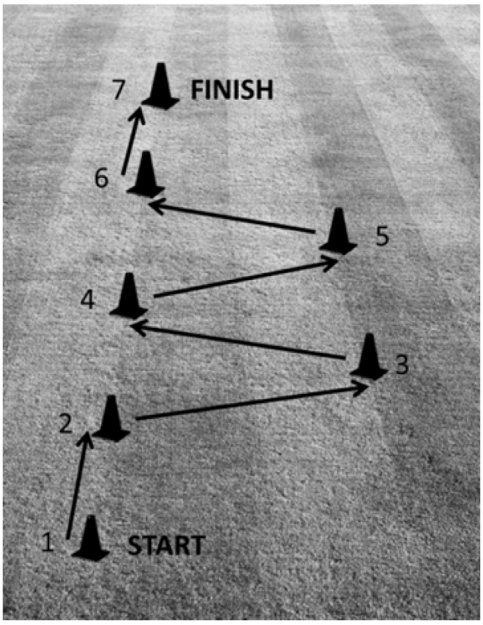

Fig. 1. Agility run course composed of 5 changes of direction. Consecutive cones spaced 5 m apart.

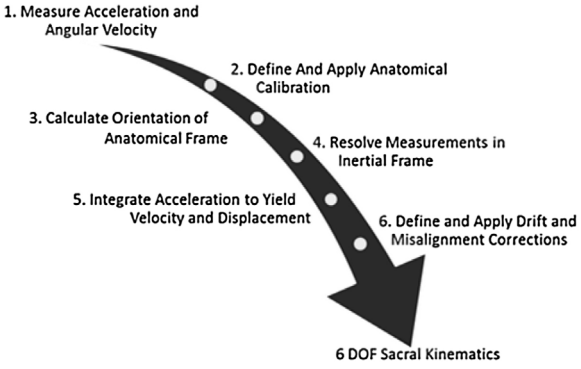

Fig. 2. High level summary of data reduction steps.

2.2. Measurement and estimation of sacral kinematics

The motion of each subject was tracked using a belt-worn inertial measurement unit (APDM Opal, Portland, OR, USA) as they completed the slalom course. The IMU measures three components of linear acceleration (a_M) and angular velocity (ω_M) in a body-fixed frame F_M characterized by the orthonormal vector triad (X_M, Y_M, Z_M, see Fig. 3) and assumed to originate from the subject's sacrum with the Y_M axis constrained to the sagittal plane, but an otherwise arbitrary orientation relative to the body. This data was sampled at 128 Hz, and low pass filtered using a 4th order Butterworth IIR filter with a cutoff frequency of 15 Hz prior to use. The time when the subject starts and finishes the slalom run is indicated in the data using a synchronized trigger that provides a unit pulse in a single data stream when a button is pressed by the study staff. We employ the IMU data to estimate the acceleration, velocity, displacement, angular velocity, and orientation of the sacrum relative to the path followed by each subject and the cones that define the slalom course. A high level summary of the steps used to transform IMU data (Step 1) into these quantities is provided in Fig. 2.

Accelerometer data from the upright standing portion of the simple calibration routine, combined with knowledge of the IMU placement, was used to define the fixed transformation from the IMU measurement frame to an anatomical reference frame for each

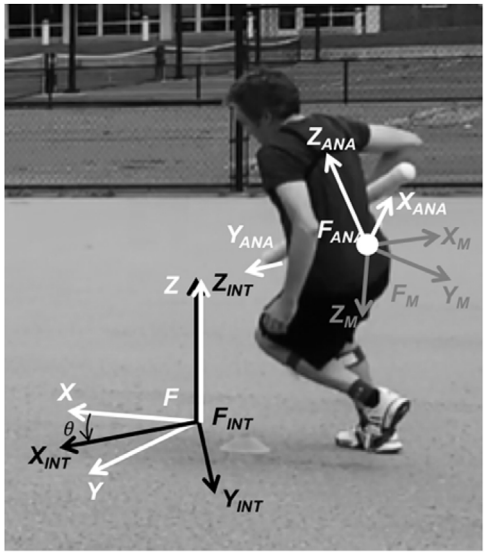

Fig. 3. Four reference frames defined in the study: measurement frame of the IMU (F_M), anatomical frame (F_{ANA}), inertial frame (F_{INT}), and course frame (F).

subject (X_{ANA}, Y_{ANA}, Z_{ANA}). As shown in Fig. 3, the anatomical frame was defined such that the axes aligned with the medial-lateral (ML, approximately X_{ANA}), anterior-posterior (AP, approximately Y_{ANA}), and longitudinal (L, approximately Z_{ANA}) axes of the subject. The transformation was then used to resolve the measured kinematics in this frame yielding a_{ANA} and ω_{ANA}.

Resolving the measured kinematical quantities in the anatomical reference frame F_{ANA} shown in Fig. 3 provides the angular velocity of the sacrum (one of our desired outputs) which is needed for determining the sacral orientation as described next.

As per Step 3 of Fig. 2, the orientation of the subject's sacrum is defined by the direction cosine matrix $C_{INT/ANA}$ which quantifies the orientation of an inertial reference frame, F_{INT}, defined by the orthonormal triad (X_{INT}, Y_{INT}, Z_{INT}, see Fig. 3), relative to the body-fixed, anatomical frame F_{ANA}. The evolution of that direction cosine matrix in time is governed by

$$\frac{d}{dt}C_{INT/ANA} = C_{INT/ANA}\omega^{\times}_{ANA} \tag{1}$$

where $\omega^{\times}_{ANA}$ is the angular velocity of F_{ANA} relative to F_{INT} represented as a skew symmetric matrix. Provided the initial orientation is known, one can integrate Eq. (1) to solve for $C_{INT/ANA}$. For this study, the initial orientation is defined using two pieces of information extracted during the period of time when the subject is still just prior to the start of the slalom run: (1) the direction of gravity measured by the accelerometer and resolved in F_{ANA}, and (2) the projection of the subject's anterior-posterior axis onto the horizontal plane. Commonly, the angular velocity in Eq. (1) is measured by an IMU (directly or following a simple calibration step) and used to compute a drift-prone estimate of orientation as a function of time, see for example [17]. Herein, we fuse this gyro-based estimate of orientation with an incomplete and noisy accelerometer based orientation estimate in a complementary filtering framework following the method presented in [18]. This yields a more accurate orientation estimate with bounded error.

We then use $C_{INT/ANA}$ to resolve a_{ANA} and ω_{ANA} in the inertial frame yielding a_{INT} and ω_{INT} per Step 4 of Fig. 2. After subtracting gravity, the difference $a_{INT} - g$ is numerically integrated forward in time once to yield a drift-polluted estimate of velocity (v_{INTd}), and a second time to yield a drift polluted estimate of displacement (d_{INTd}) from an initial condition when the sacrum is stationary and collocated with the origin per

$$v_{INTd} = \int_0^t a_{INT}(\tau) - g d\tau \tag{2}$$

$$d_{INTd} = \int_0^t v_{INTd}(\tau)\, d\tau \tag{3}$$

These estimates of velocity and displacement are corrupted by drift error, which results from numerical integration of small errors in a_{INT}. This error source has been well established as a limitation of IMUs and is the focus of considerable scientific study [see [17], for example]. To combat this problem, we pursue an approach analogous to those presented in [6,17,19,20], and assume a polynomial form for the drift error in displacement and velocity and use constraint equations on the motion to deduce the unknown coefficients of the drift error polynomials. Specifically, we assume that the drift error in displacement (e_d) and velocity (e_v) are approximated by

$$e_d(t) = c_0 + c_1 t + c_2 t^2 \tag{4}$$

$$e_v(t) = \frac{d}{dt}e_d(t) = c_1 + 2c_2 t \tag{5}$$

where c_0, c_1 and c_2, are unknown vector-valued coefficients that are unique for each trial. The corrected velocity (v_{INT}) and displacement (d_{INT}) in F_{INT} follow from

$$v_{INT}(t) = v_{INTd}(t) - (c_1 + 2c_2 t) \tag{6}$$

$$d_{INT}(t) = d_{INTd}(t) - \left(c_0 + c_1 t + c_2 t^2\right) \tag{7}$$

To estimate the unknown coefficients (c_0, c_1, c_2), we exploit the fact that each subject is completing a course with known cone locations. However, before this fact can be leveraged, we must first understand the relationship between F_{INT} and the slalom course. To this end, we define a slalom course reference frame (F) characterized by the orthonormal vector triad (X, Y, Z) with Y aligned with the start cone, the even numbered turn cones, and the finish cone; refer to Fig. 1. As shown in Figs. 3 and 6, F_{INT} is misaligned from F by an unknown rotation (θ) about vertical (Z, Z_{INT}). This misalignment is unavoidable because the orientation of F_{INT} is defined by the subject's initial posture when at rest just prior to the initiation of each agility test. Adding θ to the preceding unknown polynomial coefficients yields a total of 10 scalar unknowns (c_0, c_1, c_2, θ) that must be identified to provide drift corrected estimates of velocity and displacement.

To identify the unknowns (c_0, c_1, c_2, θ), we first identify instances during the slalom run when the subject's displacement and/or velocity is approximately known. For example, the time when the subject first starts the course (t_s) and when they pass the final cone (t_e) are both known from the trigger pulses. These time points provide three vector equations for identifying the unknowns (zero velocity and displacement at the start of the run, and known displacement at the end). Additional displacement constraints follow from knowing that the subject passes close to each cone at times when they are rapidly turning.

These 'turn times' are identified by considering the medial-lateral (ML) component of a_{ANA} (light grey curve in Fig. 4). First, we low-pass filter the ML acceleration (dark grey curve in Fig. 4) with a cut-off frequency $f = 1.5 \times \text{nturns}/t_c$, where $t_c = t_e - t_s$ is the time to complete the course and "nturns" is the number of turns. We then center the filtered ML acceleration and identify consecutive peaks (black dots in Fig. 4) using a simple state machine. We confirmed that these time points occur at approximately the instants

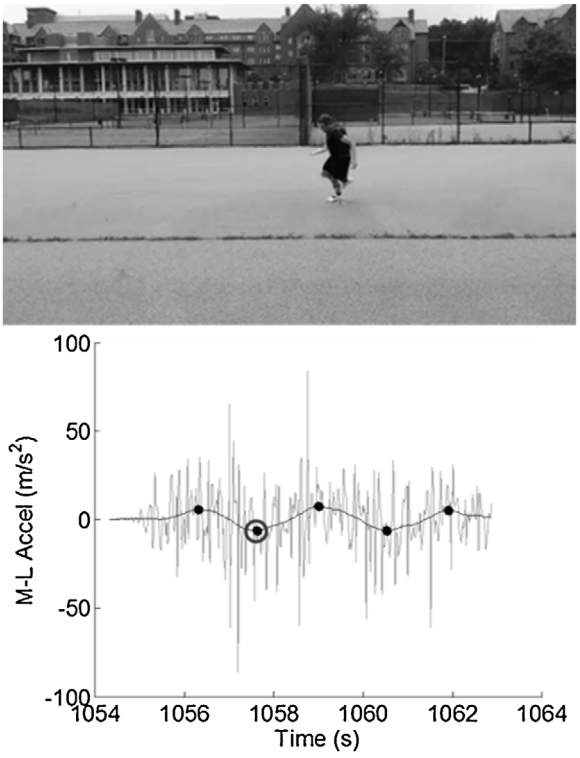

Fig. 4. Medial-lateral acceleration signal (light grey) is low-pass filtered (dark grey) and then used to identify subject turns. Black dots indicate turn times, and the circled turn aligns with the synchronized video frame above.

the subject was closest to each cone using synchronized video as shown in the sample video frame of Fig. 4.

From the five turn times ($t_i, i = 1, 2, \ldots, 5$), we define the following cost function that defines the squared error between the estimated position of the subject's sacrum and the cones at the turn times.

$$g(c_0, c_1, c_2, \theta) = \sum_{i=1}^{5} \left[d(t_i) - d_c(i) - C\left(\theta\right) e_d(t_i) \right]^2 \quad (8)$$

Here $C\left(\theta\right)$ is the direction cosine matrix describing the mapping between F_{INT} and F, $d(t_i)$ is the misalignment-corrected displacement (defined as $d = C\left(\theta\right) d_{INT}$) of the subject at the i^{th} turn time, and $d_c(i)$ is the known location of the i^{th} cone. Optimal values of the unknown constants ($c_0,\ c_1,\ c_2,\ \theta$) are found by minimizing (8) while satisfying zero velocity and displacement constraints at the starting time t_s, and the displacement constraint at the ending time t_e at the final cone location. This optimization is performed in Matlab (Mathworks, Natick, MA, USA) using separable least squares.

2.3. Performance metrics and cluster analysis

We now identify different techniques used by subjects in the slalom run by quantifying how subjects negotiate a turn. We choose to focus on the turns, as this aspect is what differentiates a test of agility from a test of speed. To this end, we first utilize the drift-corrected path and velocity to construct the normal (n) and tangential (t) path coordinate directions at each turn (Fig. 5). We then project sacral kinematic measures onto these directions leading to the turn technique metrics listed in Table 1. These metrics were selected to capture the full 6 degree-of-freedom (rotation: α_t, α_n, φ; translation: α_n, α_t, $|v_h|$) motion of the subject as they negotiate the turns in the course while also representing parameters that we felt subjects may be able to adjust with some simple technique

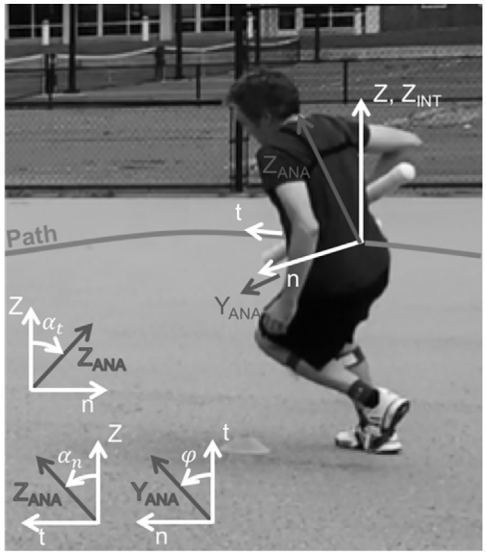

Fig. 5. Definition of the normal and tangential path coordinates and rotational turn metrics ($\varphi, \alpha_t, \alpha_n$) that characterize the technique employed by subjects when negotiating the turns in the agility run course.

Table 1
Turn technique metrics.

Feature	Description
a_n	Acceleration component normal to the subject's path at the sampled turn time
a_t	Acceleration component tangential to the subject's path at the sampled turn time
$\lvert v_h \rvert$	Speed in the horizontal plane at the sampled turn time
α_t	Absolute value of the tilt angle corresponding to sacral rotation about an axis tangential to the subject's path at the sampled turn time
α_n	Tilt angle corresponding to sacral rotation about an axis normal to the subject's path at the sampled turn time
φ	Absolute value of the angle between the projection of the anterior direction of the sacrum onto the horizontal plane and an axis tangential to the subject's path at the sampled turn time

changes (i.e. body positioning, acceleration, deceleration, and timing thereof). Fig. 5 provides definitions of the normal and tangential coordinate directions and rotational turn technique metrics.

These metrics are sampled at each turn, for each subject, and then averaged across all turns in the course. Groups in the data are identified via k-means cluster analysis, and distinction between groups is confirmed via silhouette plot [21]. Differences in the feature values between groups, and across load, are assessed using Welch's t-tests. Statistical significance is evaluated at the $\alpha = 0.05$ level.

3. Results

Fig. 6 illustrates the magnitude of the displacement drift error accrued over approximately 10 s. The black dots indicate the difference between the uncorrected displacement in the X and Y directions and the location of each cone at the turn times. The drift error estimates in the X and Y directions are shown as the dark and light grey curves, respectively.

Subtraction of these drift errors from the uncorrected displacement yields the corrected estimate of the sacral trajectory. The trajectory in the horizontal plane for this trial is shown in Fig. 7 (dark grey), where turn times are indicated by black dots, and cone locations by black circles. The associated misalignment angle, θ, is also illustrated for reference.

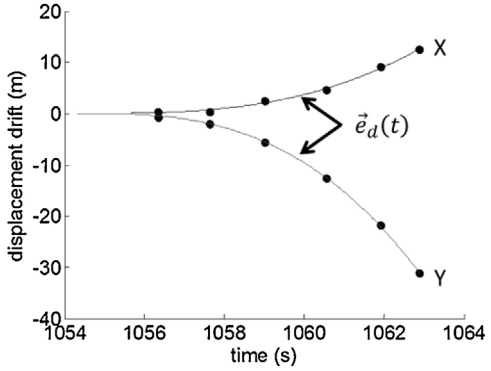

Fig. 6. Example drift error (black dots) and the functions used to approximate it in the X (dark grey) and Y (light grey) directions for one example bout of the slalom run course.

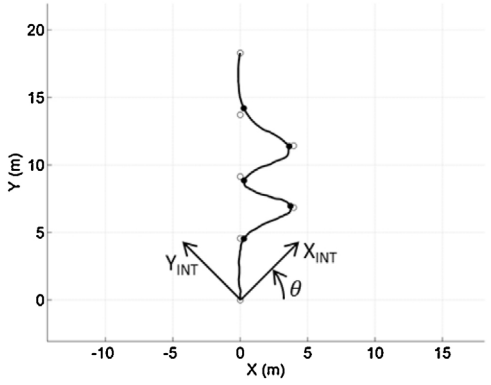

Fig. 7. Drift- and misalignment-corrected displacement of the sacrum in the horizontal plane for one representative trial. Cones are identified as black (open) circles while times identified as turns are shown with black dots.

Provided the corrected estimates of sacral displacement, velocity and acceleration, we compute the turn metrics itemized in Table 1. The k-means cluster analysis of the turn metrics reveals two distinct subject groups. Fig. 8a illustrates the mean value for each metric for Group 1 (light grey) and Group 2 (dark grey), where significant differences are immediately apparent. Fig. 8b is the silhouette plot that confirms this difference. Generally, two groups are considered distinct if the majority of silhouette values are larger than 0.6 [22].

Table 2
Average metrics across, and difference (Δ) between, groups. Difference assessed with *t*-tests, t-score (t) and *p*-value (p) reported.

Feature	Group 1	Group 2	Δ	*t*	*p*
t_c (s)	9.85	9.91	−0.06	0.16	0.87
a_n (m/s^2)	4.83	4.89	−0.06	0.13	0.90
a_t (m/s^2)	0.81	−0.22	1.03*	−4.48	<0.01
$\|v_h\|$ (m/s)	2.54	2.42	0.12	−1.21	0.25
α_t (deg)	23.35	21.88	1.48	−1.05	0.31
α_n (deg)	15.47	2.45	13.02*	−5.63	<0.01
φ (deg)	8.44	26.59	−18.15*	8.19	<0.01

* Statistically significant at the $\alpha = 0.05$ level.

Table 3
Average metrics across, and difference (Δ) between, load conditions for Group 1. Difference assessed with *t*-tests, t-score (t) and *p*-value (p) reported.

Feature	Loaded	Unloaded	Δ	*t*	*p*
t_c (s)	10.83	9.85	0.98*	5.74	<0.01
a_n (m/s^2)	4.42	4.83	−0.41	−1.12	0.30
a_t (m/s^2)	0.25	0.81	−0.56*	−3.16	0.01
$\|v_h\|$ (m/s)	2.26	2.54	−0.29*	−3.45	0.01
α_t (deg)	21.42	23.35	−1.93	−0.93	0.38
α_n (deg)	8.17	15.47	−7.30*	−4.96	<0.01
φ (deg)	16.58	8.44	8.15	2.10	0.07

* Statistically significant at the $\alpha = 0.05$ level.

The mean value for each metric and the time to complete the course (t_c), in Group 1 (n = 23) and Group 2 (n = 9), are reported in Table 2. We also report the difference between the groups and the results of *t*-tests of the significance of that difference (t-score and *p*-value).

The application of a 20.5 kg load causes significant changes in the technique employed by subjects that manifest as changes in the turn metrics itemized in Table 1 for each group. The mean value for each metric and the time to complete the course in the unloaded and loaded conditions are reported for Groups 1 and 2 in Tables 3 and 4, respectively. We also report the difference between the load conditions and the results of *t*-tests of the significance of that difference (t-score and *p*-value) in each table.

Technique changes occur across load within each group, however, these changes differ across groups, and ultimately yield the mean values for Group 1 (light grey) and Group 2 (dark grey) illustrated in the spider plot of Fig. 9. There are no longer any significant differences between the two groups in any of the turning technique metrics.

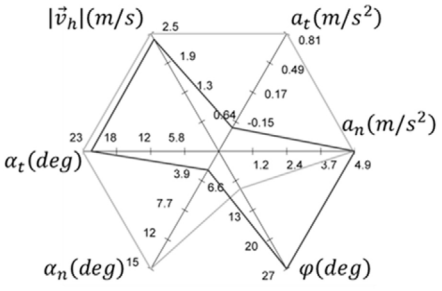

(a)

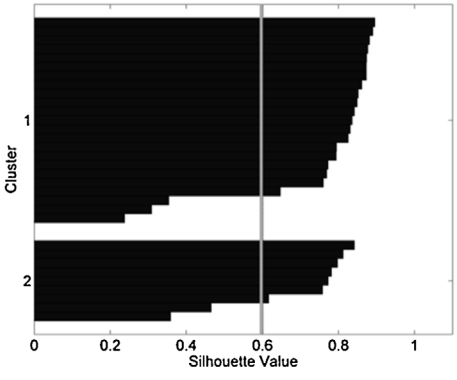

(b)

Fig. 8. Spider plot of the average turn technique metrics (a) across each of the groups (dark and light grey) identified in our dataset. Distinction between the groups confirmed via silhouette plot (b).

Table 4
Average metrics across, and difference (Δ) between, load conditions for Group 2. Difference assessed with *t*-tests, t-score (t) and *p*-value (p) reported.

Feature	Loaded	Unloaded	Δ	*t*	*p*
t_c (s)	10.91	9.91	1.00*	5.31	<0.01
a_n (m/s^2)	4.43	4.89	−0.46*	−3.08	0.01
a_t (m/s^2)	0.40	−0.22	0.62*	3.92	<0.01
$\|v_h\|$ (m/s)	2.37	2.42	−0.05	−0.75	0.46
α_t (deg)	20.58	21.88	−1.30	−1.49	0.15
α_n (deg)	3.80	2.45	1.35	0.96	0.35
φ (deg)	19.36	26.59	−7.23*	−3.17	<0.01

* Statistically significant at the $\alpha = 0.05$ level.

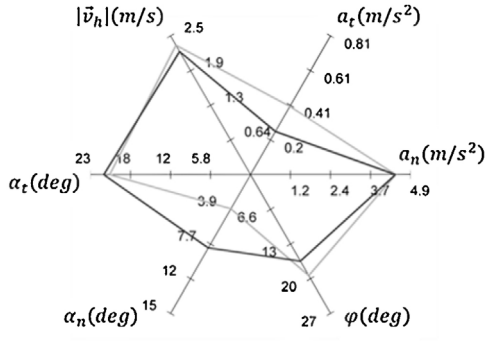

Fig. 9. Spider plot of the average turn technique features for Group 1 (light grey) and Group 2 (dark grey) when completing the course under load.

4. Discussion

This study presents a methodology for quantifying the biomechanical metrics underlying speed and agility performance in agility assessment tasks. In so doing, we describe a drift correction algorithm for tracking the displacement, velocity, and acceleration of the sacrum as a subject traverses a course with known waypoints. We demonstrate its utility by extracting kinematic quantities indicative of turning technique, using them to identify two groups within our dataset via k-means cluster analysis, and examining the differences in the techniques employed by each group. We follow this analysis with an examination of how these parameters change with the addition of a 20.5 kg load within each group, and how these changes influence group differences.

As evidenced in Fig. 6, double integration of acceleration to yield displacement results in drift errors on the order of 30 m even over the relatively short time (<10 s) it takes to complete the slalom course. The proposed drift correction algorithm produces reasonable results as shown by the trajectory (dark grey) in Fig. 7. We note that a limitation of the current study is the lack of quantitative comparison to a gold standard measure of displacement (i.e. optical motion capture) and doing so remains an interesting future study for the authors.

Nevertheless, the drift correction provides estimates of acceleration, velocity, and displacement that, when combined with the angular velocity and orientation of the sacrum, yield a full description of sacral motion. We utilize this information to examine the turning kinematics employed during the slalom run through the performance metrics of Table 1. We emphasize that this full kinematic description could be used to quantify performance in alternative agility tests with known waypoints (i.e., 5-10-5 Agility Run, 3 Cone Drill, etc.).

The spider plot of Fig. 8a and the mean performance metrics of Table 2 illustrate how the differences in technique across the groups manifest as statistically significant differences in performance at the turns. Specifically, in comparison to Group 2 (dark grey), Group1 (light grey) is characterized by a positive tangential acceleration, more pronounced forward tilt of the sacrum, and closer alignment between the instantaneous direction of travel and the anterior direction of the sacrum (φ). In contrast, Group 2 exhibits a negative tangential acceleration (braking), more upright sacrum, and greater misalignment between the direction of travel and the anterior direction of the sacrum (φ) at the turn times. These turn times correspond to local maxima or minima of the low pass filtered ML acceleration (Fig. 4). The turning technique that subject's employ ultimately dictates the phase relationship between motion in the frontal and sagittal planes, and the orientation of the pelvis, as characterized by the pelvis angles (φ, α_n, α_t), determines how the kinematic quantities within each of these anatomical planes are projected onto the normal and tangential path coordinates (i.e. α_n and α_t). All subjects likely progress through the same sequence of events to complete each turn during the slalom course including a deceleration in the tangential direction (negative α_t), a shift of the pelvis to be more upright in the sagittal plane and more tilted in the frontal plane, and an increase in the magnitude of the normal acceleration, followed by an acceleration in the tangential direction (positive α_t), a shift of the pelvis to be more tilted in the sagittal plane and more upright in the frontal plane, and a decrease in the magnitude of the normal acceleration. However, the relative timing of these changes, and how they relate to the local maxima/minima in the ML acceleration, differs between groups and ultimately yields the mean differences reported in Fig. 8a and Table 2.

At the sampled turn instants, subjects in Group 1 are already accelerating forward (positive tangential acceleration) and have aligned their hips more closely with their instantaneous direction of travel (i.e. smaller φ), as defined by the instantaneous velocity vector. This suggests that these subjects should be able to increase their speed more quickly coming out of the turn. Based on this characterization, subjects in Group 1 would be more likely to complete the course in shorter time and with higher average speed. However, these differences do not manifest as measureable differences in the time to complete the obstacle (t_c) or average speed across the turns ($|v_h|$). This could be due to a number of factors including a lack of sensitivity of agility run performance to the turning technique parameters we identified in the relatively homogenous sample considered in this analysis. Importantly, however, these results highlight the fact that the group differences exposed through this analysis would not have been identified based on completion times (t_c) alone. Characterization of technique differences is important because it could enable insight into technique deficits, tailoring of training plans to most efficiently improve performance, and identifying potentially at-risk techniques before injuries occur, all of which remain interesting future studies enabled by the IMU-based methods presented herein.

We explore the utility of tracking subject technique by examining changes within each of our turn-technique groups following application of a 20.5 kg load. As expected, subjects in Groups 1 and 2 each took significantly longer to complete the slalom run in the loaded condition (an average of 0.98 and 1.00 s longer for each group, respectively). Compared to the unloaded condition, subjects in Group 1 exhibited a decrease in their tangential acceleration, a decrease in the forward tilt of the sacrum (they were more upright), and a decrease in horizontal speed at the apex of each turn. In contrast, when compared to the unloaded condition, subjects in Group 2 exhibited a decrease in their normal acceleration, an increase in tangential acceleration, and a decrease in misalignment between the direction of travel and the anterior direction of the sacrum (φ) at the apex of each turn.

This analysis is interesting as it highlights technique dimensions along which subjects are likely to change. In this case, the combination of the unloaded technique and constraints imposed by the slalom run cause subjects in Groups 1 and 2 to adapt to the load in unique ways. For Group 1, changes occurred along the tangential

acceleration, normal tilt, and horizontal speed dimensions, which yields what seems to be a decrease in turning performance. This could be caused by a change in phasing between ML acceleration and these path-based quantities, where the subjects are reaching the apex of the turn earlier in the turning process under load than they did in the unloaded condition. In contrast, subjects in Group 2 exhibit near equal, but opposite changes along the normal acceleration and tangential acceleration dimensions along with better alignment between their hips and the direction of travel at the sampled turn instant. These changes could be related; if you hold the horizontal acceleration magnitude fixed, a change in φ would likely yield a reorientation of the acceleration vector relative to the path, and therefore near equal and opposite changes in tangential and normal accelerations. These changes made by subjects in Group 2 would suggest a potential improvement in performance or at least less performance loss across load, and especially in comparison to subjects from Group 1.

These respective changes yield the mean values of each turning metric within each group illustrated in the spider plot of Fig. 9. The unique changes that occur across load within each group erase the significant differences that existed between groups in the unloaded state. This result could indicate that the challenging load carriage task limits turning technique options for subjects, where significant deviation from the mean features reported in Fig. 9 would yield loss of balance or stability and thereby reduced performance. This has important implications for load carriage assessments, as it shows that testing in an unloaded state does not necessarily yield results that can be extrapolated to a loaded state, but it could enable prediction of biomechanical adaptation to an applied load.

5. Conclusions

We present an IMU-based method for quantifying the biomechanical metrics underlying speed and agility performance in agility assessment tasks. To this end, we describe a drift correction algorithm that enables tracking of a subject's sacral displacement, velocity, and acceleration as they traverse a course with known waypoints. We demonstrate the utility of this data by identifying performance metrics that discriminate two groups in our dataset (N = 32) who use different techniques for negotiating the turns in a slalom run in an unloaded condition. These technique groups each adapt differently to application of a 20.5 kg load, which acts to erase group technique differences under load. This method for quantifying technique, and the analysis of an applied load condition, could identify specific athletes or warfighters who need additional technique training or who need to target specific strength or balance areas to enable these techniques. More broadly, we believe that the methodology presented herein can be used widely for agility assessment to provide athletes, trainers and researchers with actionable data to inform training plans and equipment modifications in the future.

Acknowledgments

Funding provided by the US Army Natick Soldier Research, Development and Engineering Center (W911QY-13-C-0011).

References

[1] C.E. Pandorf, B.C. Nindl, S.J. Montain, J.W. Castellani, P.N. Frykman, C.D. Leone, E.A. Harman, Reliability assessment of two militarily relevant occupational physical performance tests, Can. J. Appl. Physiol. 28 (February (1)) (2003) 27–37.
[2] M.F. Heller, J.H. Challis, N.A. Sharkey, Changes in postural sway as a consequence of wearing a military backpack, Gait Posture 30 (July (1)) (2009) 115–117.
[3] K.G. Holt, R.C. Wagenaar, M. Kubo, M.E. LaFiandra, J.P. Obusek, Modulation of force transmission to the head while carrying a backpack load at different walking speeds, J. Biomech. 38 (August (8)) (2005) 1621–1628.
[4] A.K.L. Treloar, D.C. Billing, Effect of load carriage on performance of an explosive, anaerobic military task, Mil. Med. 176 (September (9)) (2011) 1027–1031.
[5] S.-C. Yen, G.M. Gutierrez, W. Ling, R. Magill, A. McDonough, Coordination variability during load carriage walking: can it contribute to low back pain? Hum. Mov. Sci. 31 (October (5)) (2012) 1286–1301.
[6] R.S. McGinnis, S.M. Cain, S.P. Davidson, R.V. Vitali, N.C. Perkins, S.G. McLean, Quantifying the effects of load carriage and fatigue under load on sacral kinematics during counter movement vertical jump with IMU-based method, Sports Eng. 19 (October (1)) (2015) 21–34.
[7] J.M. Sheppard, W.B. Young, Agility literature review: classifications, training and testing, J. Sports Sci. 24 (September (9)) (2006) 919–932.
[8] J.R. Rebula, L.V. Ojeda, P.G. Adamczyk, A.D. Kuo, Measurement of foot placement and its variability with inertial sensors, Gait Posture 38 (September (4)) (2013) 974–980.
[9] R.S. McGinnis, S.M. Cain, S. Tao, D. Whiteside, G.C. Goulet, E.C. Gardner, A. Bedi, N.C. Perkins, Accuracy of femur angles estimated by IMUs during clinical procedures used to diagnose femoroacetabular impingement, IEEE Trans. Biomed. Eng. 62 (June (6)) (2015) 1503–1513.
[10] T. Seel, J. Raisch, T. Schauer, IMU-based joint angle measurement for gait analysis, Sensors 14 (April (4)) (2014) 6891–6909.
[11] E. Bergamini, P. Picerno, H. Pillet, F. Natta, P. Thoreux, V. Camomilla, Estimation of temporal parameters during sprint running using a trunk-mounted inertial measurement unit, J. Biomech. 45 (April (6)) (2012) 1123–1126.
[12] J.B. Lee, R.B. Mellifont, B.J. Burkett, The use of a single inertial sensor to identify stride, step, and stance durations of running gait, J. Sci. Med. Sport 13 (March (2)) (2010) 270–273.
[13] S.M. Cain, R.S. McGinnis, S.P. Davidson, R.V. Vitali, N.C. Perkins, S.G. McLean, Quantifying performance and effects of load carriage during a challenging balancing task using an array of wireless inertial sensors, Gait Posture 43 (2016) 65–69.
[14] D.H. Titterton, J.L. Weston, Strapdown Inertial Navigation Technology, 2nd edition, Institution of Electrical Engineers, Stevenage, UK, 2004.
[15] R. Takeda, S. Tadano, A. Natorigawa, M. Todoh, S. Yoshinari, Gait posture estimation using wearable acceleration and gyro sensors, J. Biomech. 42 (November (15)) (2009) 2486–2494.
[16] R.S. McGinnis, S.M. Cain, S.P. Davidson, R.V. Vitali, S.G. McLean, N.C. Perkins, Inertial sensor and cluster analysis for discriminating agility run technique, IFAC-Pap. 48 (20) (2015) 423–428.
[17] R.S. McGinnis, N.C. Perkins, A highly miniaturized, wireless inertial measurement unit for characterizing the dynamics of pitched baseballs and softballs, Sensors 12 (August (9)) (2012) 11933–11945.
[18] R.S. McGinnis, S.M. Cain, S.P. Davidson, R.V. Vitali, S.G. McLean, N.C. Perkins, Validation of Complementary Filter Based IMU Data Fusion for Tracking Torso Angle and Rifle Orientation, Presented at the ASME 2014 International Mechanical Engineering Congress and Exposition, Montreal, QC, 2014, p. V003T03A052.
[19] K. King, J. Hough, R. McGinnis, N. Perkins, A new technology for resolving the dynamics of a swinging bat, Sports Eng. 15 (1) (2012) 41–52.
[20] K. King, N.C. Perkins, H. Churchill, R. McGinnis, R. Doss, R. Hickland, Bowling ball dynamics revealed by miniature wireless MEMS inertial measurement unit, Sports Eng. 13 (October (2)) (2010) 95–104.
[21] P.J. Rousseeuw, Silhouettes: a graphical aid to the interpretation and validation of cluster analysis, J. Comput. Appl. Math. 20 (1987) 53–65.
[22] S.M. AqilBurney, H. Tariq, K-means cluster analysis for image segmentation, Int. J. Comput. Appl. 96 (2014) 1–8.